Dissociating retina- and face-centered reference frames of human face recognition.

Helene Dumont[1], Valérie Goffaux[1,2]

[1] Psychological Sciences Research Institute (IPSY), UCLouvain, Louvain-la-Neuve, Belgium

[2] Institute of Neuroscience (IoNS), UCLouvain, Louvain-la-Neuve, Belgium

Corresponding Author : Valérie Goffaux

valerie.goffaux@uclouvain.be

Psychological Sciences Research Institute
Place Cardinal Mercier 10/L3.05.01
1348 Louvain-la-Neuve,
Belgium

Abstract

Face identity recognition is a core function of the human brain, predominantly driven by horizontally-oriented facial cues. While face processing largely operates in a face-centered reference frame, it is not devoid of retinotopic sensitivity. Addressing whether face rotation influences the orientation tuning profile of identity recognition enables a direct empirical test of the reference frame of human face identification.

Forty-two young adults performed identity recognition of famous faces filtered to restrict content to narrow orientation bands (i.e., from 0° to 150°, in 30°-steps), and presented either upright, rotated by ±45°, or by ±90° away from upright. If the horizontal face identity information is defined along face-centered coordinates, identity recognition performance should stay tuned to the horizontal irrespective of rotation angle. The contribution of the retina-centered reference frame should cause the peak of orientation tuning to shift away from the horizontal, in the same direction as the stimulus rotation.

While overall identity recognition performance decreased when faces were rotated by ±90° compared to upright and ±45° rotation, it kept broadly tuned to the horizontal range of the face stimulus regardless of rotation angle. However, the advantage of the horizontal over the vertical range decreased significantly for ±90° compared to upright and ±45° rotations.

Through the systematic investigation of the orientation tuning parameters across stimulus rotation, the present work provides quantitative evidence that the visual information driving human face-specialized identity recognition is defined within the reference frame of the face-image.

Keywords: identity recognition; human face; reference frame; horizontal tuning; orientation selectivity; rotation.

Introduction

Faces abound in our visual environment and their visual processing is a pillar of human social communication (Holler, 2025). The human brain has developed visual mechanisms specialized in the perception of the rich and complex social cues conveyed by faces (e.g., gaze direction, age, identity, emotional expression, etc). In particular, visual mechanisms for identity recognition have consistently been shown to be selectively tuned to the horizontal structure of the face stimulus. For example, when humans are asked to recognize the identity of face images filtered to restrict stimulus content to a selective orientation band, recognition performance typically draws a Gaussian, peaking in the horizontal range, and reaching its minimum for vertically-filtered faces. This horizontal tuning of face processing is robust, as it has been found using diverse manipulations of image oriented content such as orientation filtering (Dakin & Watt, 2009; Dumont, Roux-Sibilon, & Goffaux, 2024; Duncan et al., 2017; Duncan et al., 2019; Goffaux & Greenwood, 2016; Pachai, Bennett, & Sekuler, 2018; Pachai, Sekuler, & Bennett, 2013; Pachai et al., 2017), noise masking (Goffaux & Dakin, 2010; Pachai, Sekuler, & Bennett, 2013; Pachai et al., 2017), phase randomization (Jacques, Schiltz, & Goffaux, 2014) as well as across various cognitive tasks such as identity recognition (Dakin & Watt, 2009; Dumont, Roux-Sibilon, & Goffaux, 2024; Pachai et al., 2017), detection (Balas, Schmidt, & Saville, 2015), and emotional expression recognition (Balas et al., 2015; Duncan et al., 2017; Huynh & Balas, 2014; Yu, Chai, & Chung, 2018).

Altogether, this past evidence suggests that the specialization and efficiency of face identity processing by the human brain relies on orientation-dependent visual mechanisms and, more specifically, on the processing of horizontally-oriented face cues. Yet this characterization of the visual information supporting the essential function of face identity recognition is missing one key insight: its reference frame. It is elusive whether the horizontal information driving human face identification is best defined in egocentric coordinates, namely with respect to the observer's retina, or in allocentric coordinates, with respect to the vertical elongation axis of the face stimulus. Indeed, retina and face-centered reference frames have been confounded in past investigations of the horizontal tuning of face recognition as face stimuli were typically presented upright (or inverted) to observers sitting head-straight in front of the computer screen (See Figure 1 top).

A reference frame fully centered on the retina would imply that the horizontal face identity information is determined in retinotopic visual areas like V1. Such a purely retinotopic code is very unlikely (Duncan et al., 2019; Jacobs et al., 2020). Indeed, face inversion in the image plane and contrast negation both disrupt the horizontal tuning of human face recognition despite maintaining the alignment of face- and retina-centered coordinates (Dumont, Roux-Sibilon, & Goffaux, 2024; Goffaux & Dakin, 2010; Goffaux & Greenwood, 2016; Pachai et al., 2017). Moreover, past evidence indicates that the horizontal tuning of face perception emerges in high-level regions of the ventral visual pathway (Goffaux et al., 2016; Jacques, Schiltz, & Goffaux, 2014), which are traditionally conceptualized as largely position-invariant. Altogether, this evidence indicates that the reliance on face horizontal information predominantly arises in high-level mechanisms tuned to the statistical properties of the *upright* human face and is not primarily driven by retinotopic mechanisms.

Yet, while high-level visual representations of e.g. faces are commonly thought to be defined in an object-centered, position-invariant, coordinate system, more recent work hints that high-level face processing is not completely devoid of retinotopic sensitivity (Afraz & Cavanagh, 2008; Groen et al., 2022; Morsi, Goffaux, & Greenwood, 2024; Roux-Sibilon et al., 2023). The systematic quantification of the orientation tuning parameters across stimulus rotation enables a direct test of the reference frame of the specialized, horizontally-tuned, mechanisms recruited during face identity recognition.

To investigate the contribution of retina- and face-centered reference frames to identity recognition, we filtered face images in the orientation domain and presented these images rotated in the image plane to upright-sitting observers. In these conditions, upright (0° rotation) face images had both cardinal axes aligned with those of the observer retina's while rotating the face image (by 45° or 90°) misaligned image and retina axes proportionally to the angle of its rotation. By comparing the orientation tuning profile of identity recognition performance of orientation-filtered faces at different rotation angles, we were able to determine the reference frame(s) contributing to the advantage of horizontal information for face recognition. A strictly face-centered reference frame predicts that recognition performance remains tuned to the face-centered horizontal range, no matter the rotation angle of the face stimulus. A strict retinotopic reference frame instead implies a shift of the orientation tuning peak equal to the face rotation angle. For instance, with faces rotated by 45°, recognition performance would be best for faces filtered with a filter centered on 135° (i.e., adding 90° for the horizontal filter and +45° for face rotation = 135°; Figure 1 bottom). However, considering the evidence reviewed above, a more nuanced pattern where the peak of the tuning curve deviates more moderately from the face-centered horizontal according to rotation angle seems more plausible. The peak location shift would enable to quantify the extent of the retinal contribution to face identity recognition.

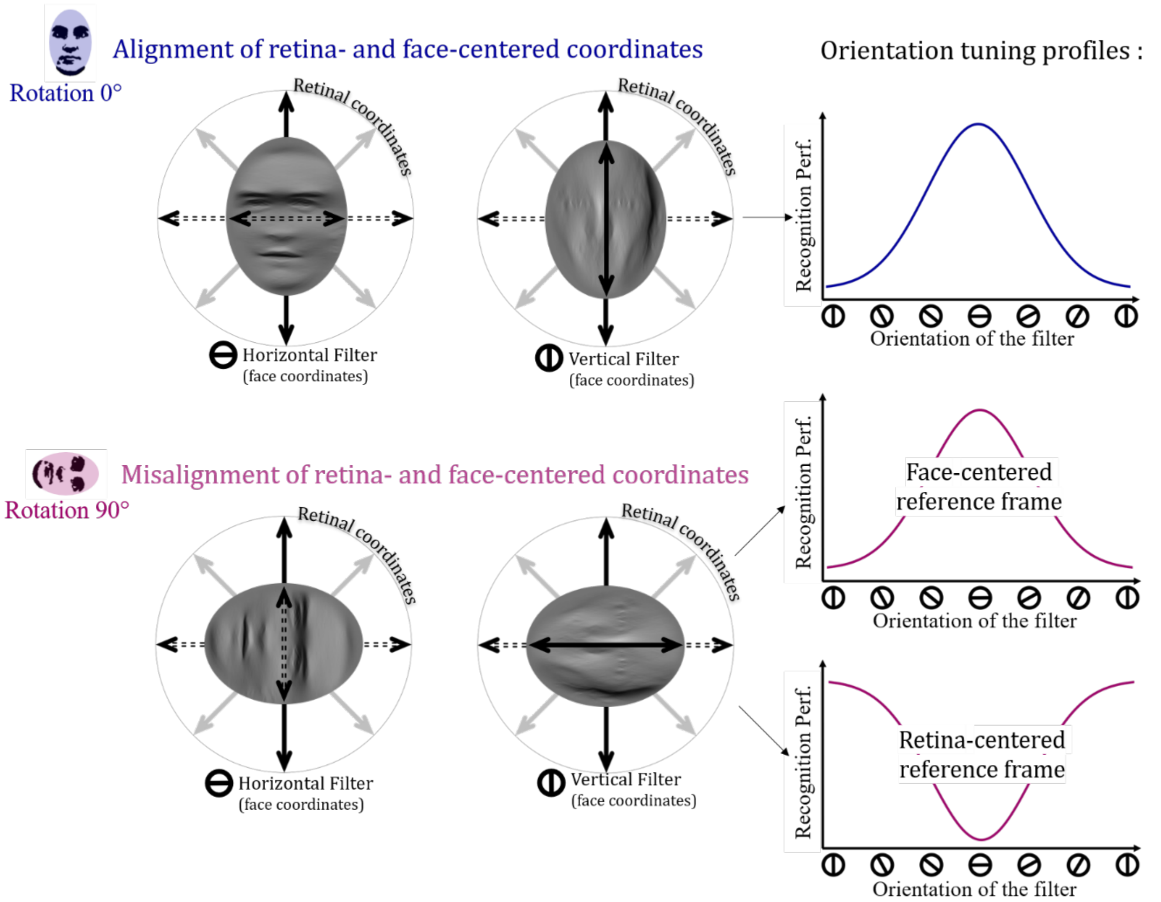

Figure 1: Left. In upright faces (0° rotation), the orientation-filtered stimulus content is aligned across the face- and retina-centered reference frames. Rotating the face stimulus away from upright misaligns the face- and retina-centered frames of reference. **Right.** Predictions of the orientation tuning profile of face recognition are presented, in the case of a strictly face-centered reference frame top) and in the case of a strictly retina-centered reference frame.

Material and Methods

Our goal was to characterize the coordinate system of the (horizontal) information driving human face recognition. To this end, we filtered faces in orientation ranging from 0° to 150° in steps of 30° (in face-centered coordinates; 0° being vertical and 90° horizontal). These images were then presented either upright or rotated by 45° and 90° (counter) clockwise, relative to the observer. Not exceeding a 90° rotation ensured the engagement of horizontally-tuned mechanisms in all conditions (e.g., Rossion & Boremanse, 2008).

Participants

A total of 46 participants were recruited via ads on Facebook groups from 02/11/23 to 10/05/24. Participants with a normal or corrected to normal vision (FrACT scores < 0 for all enrolled participants) and face recognition abilities (Benton recognition task scores; 48.56 ± 2.86) were included in the sample. A total of 42, nine males, two non-binary participants, aged 25.38 ± 3.7 completed the experiment, divided into two groups, one for each rotation direction: 25 for counter-clockwise and 17 for clockwise . Our preliminary analyses of the counter-clockwise data in 25 participants indicated that a smaller sample was sufficient to make the statistical models converge, resulting in different sample sizes across rotation directions. Before the start of the experiment participants gave their written informed consent, based on a short descriptive of the study and its goal. They were informed that they could withdraw their consent at any time. The experiments lasted for 3 sessions of approximately 1h, participants were compensated 10 euros per session. At the end of their last session participants had the opportunity to ask any question. The experimental protocol was approved by the local ethical committee (Psychological Sciences Research Institute, UCLouvain).

Stimuli

Orientation-filtered images of famous actors' faces were presented upright, rotated by 45° or 90° degrees (counter)clockwise. We used the FameSet image set as in Dumont et al. (2024). The set consists of images of famous male actors, selected through an online piloting phase on Pavlovia (Open Science Tools, Nottingham, UK), to ensure recognition from the greatest numbers of participants. The image set was composed of a total of 72 full front (or close to full front) pictures, 4 images for each identity, deprived of any distinctive accessory (such as glasses, tattoos or piercings). All actors were white American or English males. Images were grey-scaled and rotated to align the eyes with the horizontal meridian when necessary. Images were cropped to encompass the face from forehead to chin and resized to 302 x 339 pixels. Pixel values were normalized to vary between 0 and 1. We set each image mean luminance to 0.5, and RMS contrast to 0.1, all the while insuring a clipping proportion (proportion of pixel below zero or above 1) under 3%. Images were symmetrically padded to thrice their size to avoid border effect during filtering. Images were fast Fourier Transformed, and their amplitude spectra were multiplied with wrapped Gaussian filters designed to restrict image energy to narrow orientation bands. The center of the Gaussian filters ranged from 0° to 150° in steps of 30°, with a standard deviation of 20° (see Figure 2). Compared to our previous study (Dumont, Roux-Sibilon, & Goffaux, 2024), the filter's standard deviation was reduced (from 25° to 20°) to avoid ceiling performance for upright images. After the inverse Fourier Transform, the mean luminance and RMS contrast of all filtered images was again equalized to match 0.5 and 0.1. An aperture designed to broadly match the contours of the average of the face images was alpha-blended with each filtered and full spectrum image. Finally, pink noise masks (1/f) were designed to match the mean luminance and RMS contrast values of the face images. MatlabR2014a and Python3.11 were used for image processing.

All of the stimuli (face and mask images) were displayed on an isoluminant uniform grey background ([0.5, 0.5, 0.5] in RGB).

Procedure

Before starting the experiment, participants selected actors whose faces were familiar to them. The actor selection process consisted of each of the 72 images (4 images for each of the 18 identities) randomly presented in the middle of the screen for 500 ms, followed by 5 actors names (the name of the actor just presented and 4 other names, randomly selected among the 17 remaining actors). Participants had to click on the name of the actor that was just presented or on the "I don't know" button. An actor was only considered familiar if the participant recognized him in at least 3 out of the 4 images. Once the participant had recognized 10 identities, the four images of each identity were selected for the main experiment and displayed again on the monitor for five seconds. Identity selection was thus tailored to participant's personal familiarity with the face stimuli.

The main experimental task consisted in a delayed face identity matching task, similar to the one used in (Dumont, Roux-Sibilon, & Goffaux, 2024). A trial started with a white fixation point lasting randomly between 750 ms to 1350 ms, followed by a face image for 200 ms, a mask during 200 ms and the second face image during 200ms, all displayed at screen center. Participants had to press the letter "S" for same identity and "L" for different identity on the keyboard placed in front of them. Whether the pair similarity was "same" or "different" identities, the displayed images were different, to avoid reliance on image matching strategies. Answers were recorded from stimulus onset and up to 4000ms after stimulus offset. The fixation point turned to green after a correct answer and red for an incorrect answer, then back to white, after which a new trial began.

To ease task execution, trials were blocked per rotation angle (either upright, at ±45° or at ±90°). Each block was made of 14 trials, two for each filter condition (including full spectrum) and followed by a three-second break, after which a tone indicated the start of the new block. Blocks were grouped by three, one for each rotation condition, in a randomized order. Blocks were short and contained diverse orientation filter conditions, thus minimizing the risk of participants adopting compensatory strategies. After each block triplet, the accuracy score, calculated over the last block triplet, appeared as well as the block number. This screen lasted for at least 10 seconds and required participants to press the "space" bar to continue the experiment.

Before the main experiment, participants were trained to the task, first with- full spectrum upright and rotated images (rotation angle at 45° or 90°; clockwise for 17 participants, counter clockwise for the 25 others), and next with upright and rotated full spectrum as well as orientation-filtered. In order to move to the main experiment, accuracy had to be at least 80% over 42 full-spectrum trials and 75% over 42 full spectrum and orientation-filtered trials. Training was repeated until accuracy threshold was reached.

The main experiment consisted of a total of 90 blocks (30 blocks per rotation condition), giving a total of 1260 trials. There were 30 trials in each of the 42 experimental conditions: three rotation angles (0°, +45°, +90° or 0°, -45°, -90°), seven levels of orientation content (full spectrum, 0°, 30°, 60°, 90°, 120°, 150°), and two levels of pair similarity (same/different).

Stimuli were presented on a Viewpixx monitor (VPixx Technologies Inc., Saint-Bruno, Canada) with a 1920 × 1080 pixels resolution and a 70Hz refresh rate. Participants used a head-and-chin-rest to maintain head position and a viewing distance of 60 cm. Face images presented at this distance subtended a visual angle of 9° by 10.4°, which simulates face viewing at conversational distance; the masks had a diameter of 11°. The experiment lasted for three hours split into three one-hour sessions. We used Psychopy2021.2.3 to code and run the experiment.

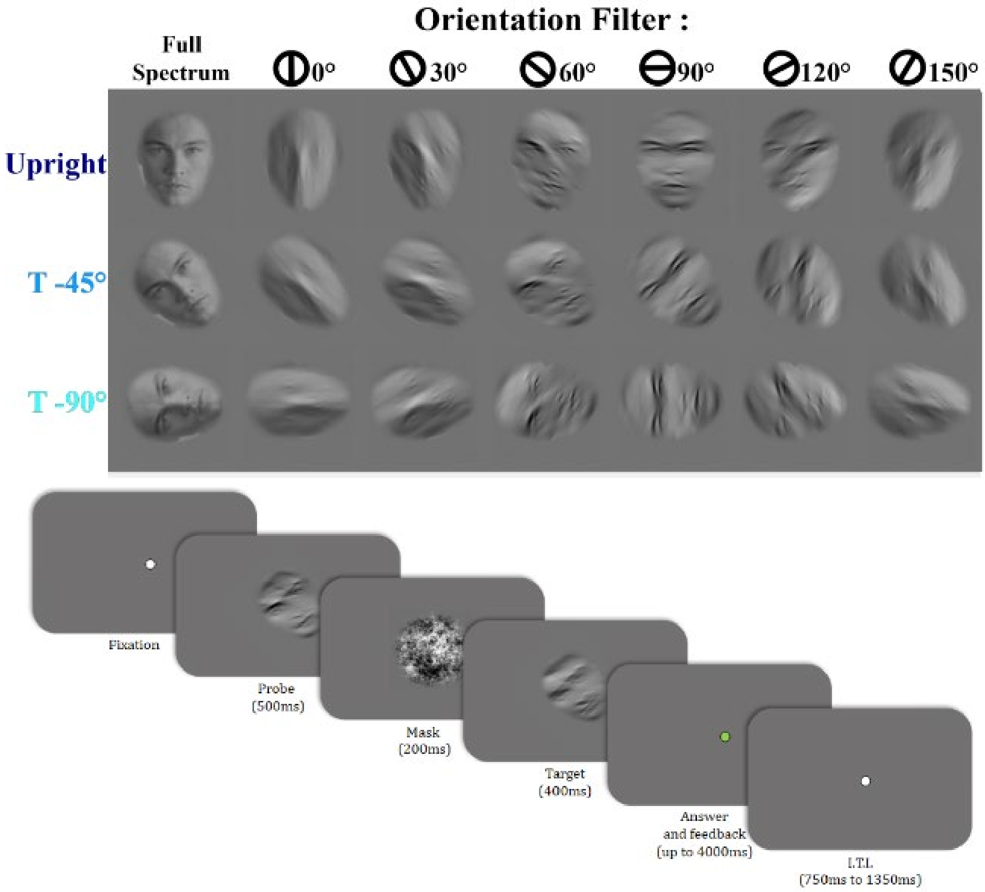

Figure 2: **Top**. Illustration of experimental conditions (filter x counter-clockwise rotation angle) with one of the images of Leonardo DiCaprio. Images are filtered from 0° to 150° in steps of 30°. The filter standard deviation is 20°. The clockwise +45° and +90° rotations are not represented. **Bottom**. Example trial with a pair of 120°-filtered face images rotated by -45° rotation. It is a *same* trial, using two different images of the same identity, here, Daniel Radcliffe.

Data analysis

To determine the reference frame of the horizontal cues to face identity, we compared the orientation tuning profile of recognition performance across stimulus rotation angles.

For each participant, we analyzed response accuracy and latency. First, we removed all participants who did not complete the full experiment in 3 sessions; this brought the final number of participants from 46 to 42. We checked that all participants scored above chance level in all conditions. Finally, to exclude outlier response, we logarithmically transformed the response time using Log_{10}, calculated its mean and standard deviation (sd) for each subject and kept only the trials in which $Log_{10}(RT)$ were included in [mean – 2.5*sd, mean + 2.5*sd], resulting in a removal of 2% of the trials overall.

We analyzed sensitivity *d'* to control for potential response bias (for accuracy analysis, see Supplementary S1). For *d'* calculation, we designated *same* answers for same identity as ***hits***, *same* answers for different identity as ***false alarms***, *different* answers for different identity as ***correct rejections*** and *different* answers for same identity as ***misses***. Hit and false alarm rates were corrected following Hautus (1995). To increase intersubject comparison across conditions and facilitate data modelling the resulting *d'* values were normalized (*normd')* with a z transform using the grand mean and standard deviation (i.e. computed across conditions and subjects). Finally, we duplicated the 0°-filter *normd'* to make the 180°-filter and center the orientation tuning profiles on the horizontal.

First, we investigated the effect of stimulus rotation angle on overall identity recognition separately in full spectrum faces and orientation-filtered (i.e., *normd'* averaged across orientation-filtered conditions) faces using a Bayesian General Linear Mixed Model (GLMM) on *normd'* with subject as a random effect and with *brms* automatic priors. The Bayesian GLMM was defined as:

$$normd' \sim \text{Rotation Angle} + (\text{Rotation Angle} \mid \text{Subject})$$

We opted for the Bayesian GLMM for the sake of consistency with the statistical analysis of the orientation tuning profiles across rotation angles (see below).

Second, we examined the orientation tuning profile of identity recognition across face rotations. Performance depicted a Gaussian distribution as a function of Orientation filter. Therefore, we fitted human sensitivity data using a nonlinear, Gaussian model. This allowed characterizing the parameters of the tuning profile, namely, peak location, peak amplitude, standard deviation and base amplitude, which are directly interpretable in cognitive/functional terms. The use of a Gaussian model is motivated by past work that showed that it fits well to the evolution of face recognition performance as a function of orientation (Dakin & Watt, 2009; Dumont, Roux-Sibilon, & Goffaux, 2024; Goffaux & Greenwood, 2016; Roux-Sibilon et al., 2025). This approach has proven its sensitivity to peak location shifts for identity recognition across views (Roux-Sibilon et al., 2025), with a similar sample size (n22), n trials per condition (40 trials), orientation filter standard deviation (20° in both studies), and comparable model diagnostics. Simpler frameworks, i.e. a linear model predicting *d'* from the interaction between orientation and viewpoint, would be difficult to analyze and interpret.

At 0° and ±45° Stimulus rotations, we noted a slight decrease of performance for the horizontal range compared to the adjacent oblique ranges (similar observation as inDumont, Roux-Sibilon, & Goffaux, 2024). Yet this departure from a perfectly Gaussian distribution did not hamper model fitting (see below).

The Gaussian model was defined as:

$$Normd' \sim Base\ Amplitude + Peak\ Amplitude * \ e^{\frac{(Orientation\ filter - Peak\ Location)^2}{2Standard\ Deviation^2}}$$

Peak location is the orientation filter at which the Gaussian-modelled recognition performance is best; standard deviation measures the sharpness of orientation tuning around the peak location; base amplitude is the minimum performance; and peak amplitude indicates the difference between minimum and maximum (i.e., peak) performance.

Next, the Gaussian parameter estimates were compared between rotation angles using their 89% credible intervals (CrI) to test for a “significant” difference. All 4 parameter estimates were defined along these linear regressions:

Peak Location ~ 1 + Rotation Angle + (1 + Rotation Angle | Subject)
Standard Deviation ~ 1 + Rotation Angle + (1 + Rotation Angle | Subject)
Base Amplitude ~ 1 + Rotation Angle + (1 + Rotation Angle | Subject)
Peak Amplitude ~ 1 + Rotation Angle + (1 + Rotation Angle | Subject)

For each of these regression models, prior distributions were defined for intercept (i.e., 1), slope (i.e. the effect of Rotation Angle), and random effect of Subjects (see Table 1 for details about the prior distributions used in the model). Intercept priors of the linear regression models were normal distributions, the means of which were chosen based on theoretical expectations and previous results. For example, the prior for Standard deviation was set at 50°, halfway between previous results from our team (Dumont, Roux-Sibilon, & Goffaux, 2024; Goffaux & Greenwood, 2016; Roux-Sibilon et al., 2025). Priors for slopes of the linear regression models were also normal distributions centered on 0 (i.e., the most probable *a priori* was that there would be no difference between the tuning curves of each rotation angle). Finally, priors for random effects were exponential distributions (i.e. positive values only, to specify that there cannot be less than zero variance between subjects; Table 1).

The prior distributions of the different parameters of the Gaussian model were specified based on a compromise between (1) knowledge from previous research (e.g. past evidence that face recognition peaks in the horizontal range; Dakin & Watt, 2009; Dumont, Roux-Sibilon, &

Goffaux, 2024; Goffaux & Greenwood, 2016; Roux-Sibilon et al., 2025), (2) keeping unbiased uncertainty when previous research was not informative (e.g., for the effect of face rotation on the different parameters), and (3) allowing the convergence of the model. These priors provided the flexibility needed to model both the fixed effects of interest and the individual differences in performance. Since the model had to fit five Gaussians, which complicated the convergence of MCMC, the priors used here were slightly more limited than in Dumont et al. (2024). Table 1 provides a detailed overview of the priors used in our regression models.

All models were fitted with four MCMC with 12,000 iterations each (4,000 warm up at each iteration, resulting in 32,000 iterations after warmup). The potential scale reduction factor (R-hat) was of 1.01 for all parameters; the Effective Sample Size (ESS) was superior to 400 (100* the number of chains) for all parameters with 2388 being the smallest. The high ESS values indicate that the posterior was well-determined by the data.

Table 1. Priors of Gaussian Bayesian mixed models. Normal prior distributions were set on parameters of linear regressions (intercept and slope) and exponential distributions were set on parameters estimating random effects.

Gaussian parameter	**Peak Location**	**Standard Deviation**	**Peak Amplitude**	**Base Amplitude**
Prior for Intercept	normal(90, 5)	normal(50, 10)	normal(1.5, 1)	normal(-1.5, 1)
Prior for slope (effect of Rotation angle)	normal(0, 5)	normal(0, 10)	normal(0, 1)	normal(0, 1)
Prior for random effects	exponential(0.1)	exponential(0.1)	exponential(0.1)	exponential(0.1)

For sake of comprehensibility, it is important to remind the reader that, in Bayesian mixed-effects analysis, “population-level” includes all participants (fixed effects), and “group-level” is used to describe the sub-categories of the multilevel analysis (random effects), here the participant level.

The analysis was done using R 4.2.2. We used the *brms* package (Bürkner, 2018a, 2018b) to fit all Bayesian models. Stimulus, data and codes for stimulus presentation and data analysis can be found at https://osf.io/zyv7b/?view_only=9dd0672a866748e5b2d489b9ec625db0.

Results

As expected, overall recognition performance (i.e., average of *normd'* across orientation filter conditions) was best for upright images and decreased progressively as a function of stimulus rotation angle (see Figure 3). The 89% CrIs reported in Table 2 show a significant difference between upright (i.e., 0° rotation) and all other rotation angles, as well as between the +45° and -45° rotations and the rest of the rotation angles. The clockwise or counter-clockwise direction of rotation did not influence overall *normd'*. Similar results were found for full spectrum images with decreasing performance as a function of face rotation (Supplementary S3).

Table 2: GLMM means and 89% Credible Intervals (CrI) of *normd'* for each rotation angle averaged across orientation filter conditions.

Rotation Angle	Mean	CrI_low	CrI_high
0°	.40	.30	.52
-45°	.01	-.07	.20
+45°	.06	-.05	.30
-90°	-.7	-.69	-.43
+90°	-.7	-.69	-.32

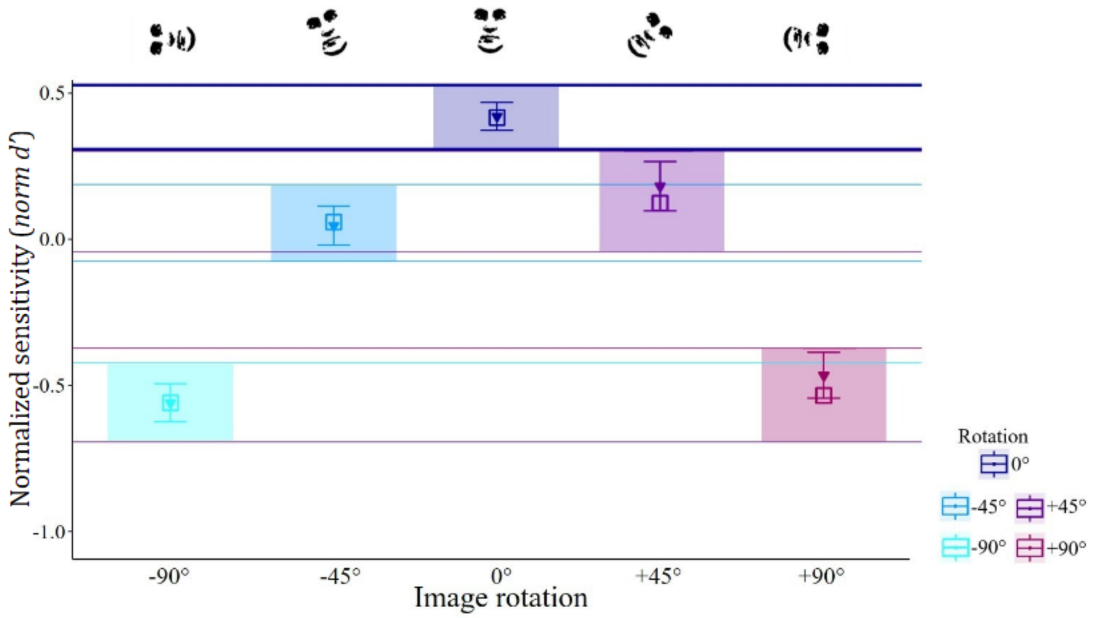

Figure 3: Predictions from the Gaussian Bayesian mixed model for each Rotation angle. Non-overlapping 89% credible intervals (CrI) of model predictions indicate significant difference. Triangles and error bars represent the means and standard errors. Squares are the model predicted means, the shaded regions and lines represent the 89% CrI.

Besides these overall influences of stimulus rotation on recognition performance, we examined the orientation tuning profile of identity recognition performance at each rotation angle. In line with the past studies employing ambient face images (Dakin & Watt, 2009; Dumont, Roux-Sibilon, & Goffaux, 2024; Roux-Sibilon et al., 2025), group-level performance plateaued between 60° and 120° (for 0° and ±45° rotations; Figure 4 Top). Across rotation angles, human sensitivity to identity was well modelled by a broad Gaussian peaking at 90° (i.e., horizontal) progressively decreasing towards 0° (i.e., vertical) (Figure 4 Bottom; see Supplementary S1 for analyses of accuracy).

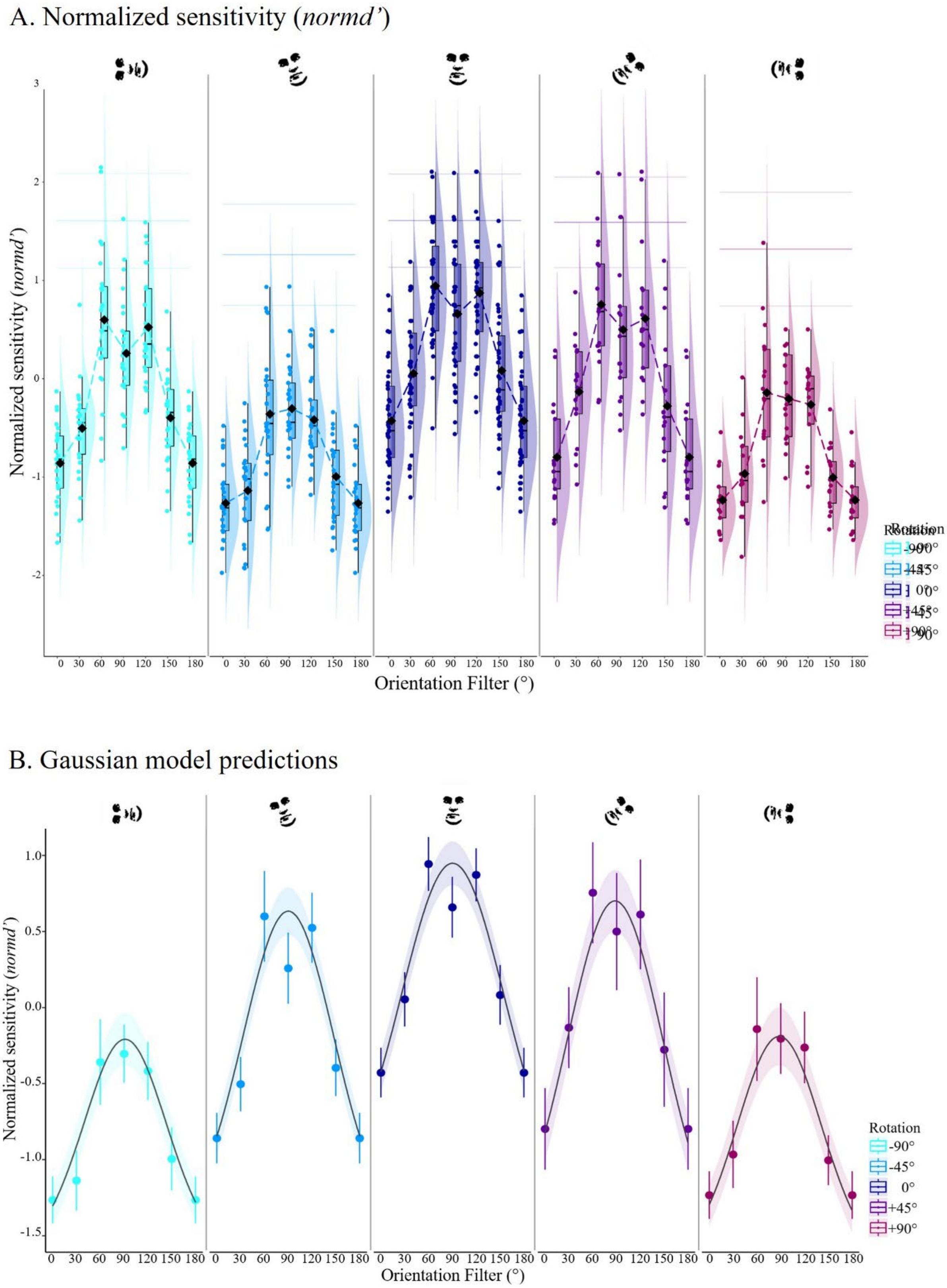

Figure 4: **A**. Group-level normalized sensitivity (*normd'*) for identity recognition as a function of orientation filters and stimulus rotation. The black diamonds represent the mean performance for each condition, and the boxplots represent the 25%, 50% (median) and 75% quantiles. Each point is one participant's recognition performance for an Orientation filter and Stimulus rotation. The half violins represent data distribution in each condition. The straight lines on top

are the *normd'*, with standard deviation in lighter lines for full-spectrum images for each Stimulus rotation. **B.** Bayesian Gaussian mixed model predictions of *normd'* for each Stimulus rotation condition. Dots represent population-level mean recognition sensitivity and error bars are 95% confidence intervals (CI). The model mean posterior predictions for each Stimulus rotation are drawn in black (line) and the 89% credible intervals (CrI) of predictions are represented as faded ribbons. *Normd'* peaked in a broad horizontal range and decreased towards the vertical orientation at all Stimulus rotation angles.

To compare the orientation tuning of face recognition across stimulus rotation angles, we analyzed the posterior parameter estimates of the Gaussian model (see Figure 5). Peak location estimates did not differ across rotation angles. The 89% CrI were all centered on the 90° filter and overlapped in-between rotation angles (see Table 3). The posterior credible interval of peak location was more narrowly distributed around horizontal than our prior (Table 3). Such reduction of uncertainty suggests that our data enabled an unbiased parameter estimation (Kruschke & Liddell, 2018). Therefore, the stability of peak location against face rotation can be taken to indicate that the horizontal information to which face recognition attunes is defined in a face-centered reference frame.

Tuning sharpness (standard deviation parameter) varied slightly, yet not significantly, across rotation angles. The selectivity of the horizontal tuning tended to be broader for upright than rotated faces. Base amplitude estimates progressively increased, although not significantly (i.e., better recognition for vertically-filtered faces) as Stimulus rotation angle approached 0°. Finally, peak amplitude estimates 89% CrIs were significantly larger for upright faces, and moderately rotated faces compared to the most extreme rotation angles (see Table 3). However peak amplitude at +90° rotation was not significantly different from -45° rotation.

To summarize, rotating faces away from upright preserves but decreases the horizontal advantage of face identity recognition.

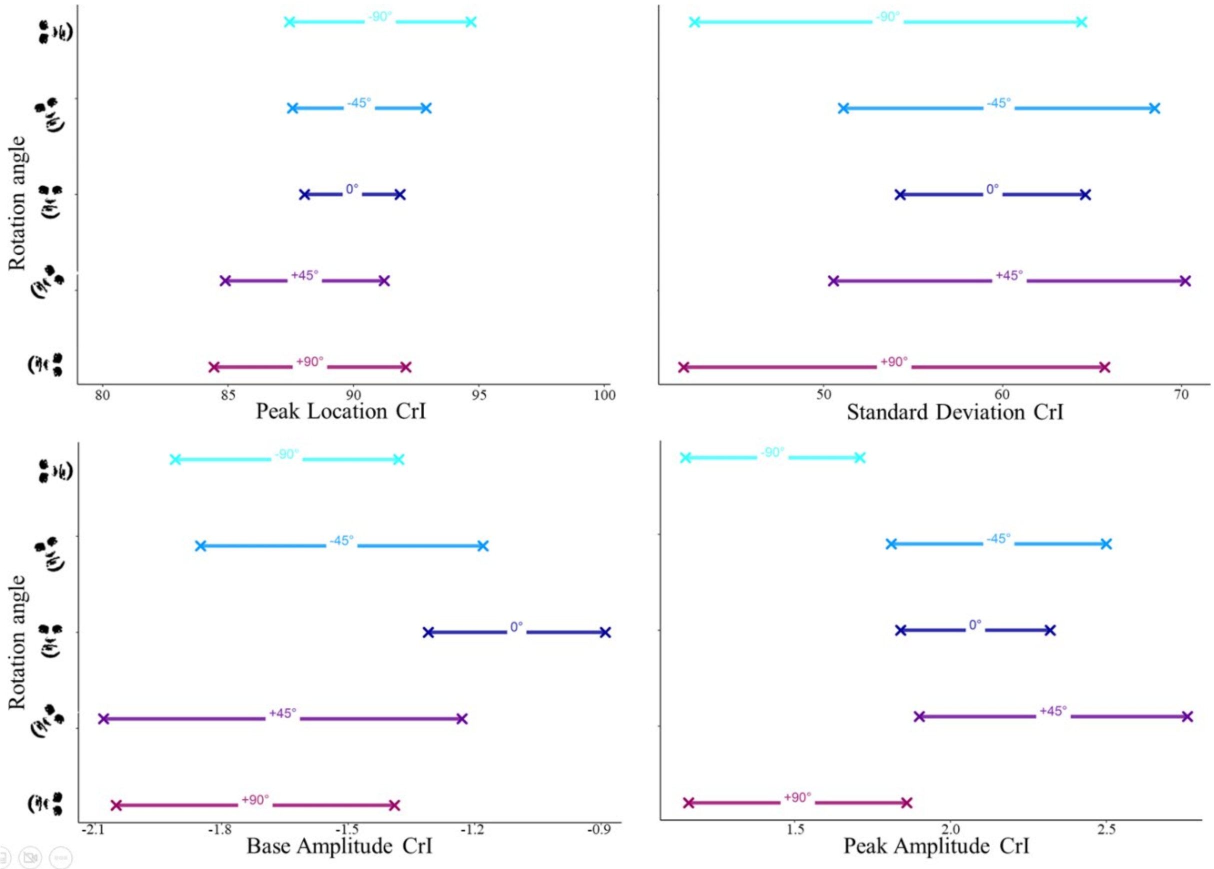

Figure 5: 89% Credible Intervals (CrI) of the Bayesian Gaussian model posterior parameter estimates across stimulus rotation angles. The only significant difference is found for the peak amplitude estimate, where the amplitude for the orientation tuning of face recognition is significantly lower for +90° and -90° rotations than for other rotation angles except for +90° and -45°.

Table 3: Gaussian parameter estimates mean, median and 89% credible intervals (CrI) for each face rotation angle.

	Peak Location (°)				Standard Deviation(°)			
	Mean	Median	CrI_low	CrI_high	Mean	Median	CrI_low	CrI_high
R -90°	91.13	91.12	87.52	94.68	52.10	52.65	41.93	63.54
R -45°	89.99	89.99	87.77	92.15	57.16	57.25	51.01	64.02
R 0°	90.19	90.19	88.06	92.34	65.02	65.31	56.57	73.82
R +45°	88.07	88.07	84.99	91.26	60.54	60.87	50.49	70.47
R +90°	88.15	88.15	84.29	91.98	53.38	53.91	42.08	65.16
	Base Amplitude				Peak Amplitude			
	Mean	Median	CrI_low	CrI_high	Mean	Median	CrI_low	CrI_high
R -90°	-1.61	-1.63	-1.89	-1.37	1.41	1.43	1.14	1.69
R -45°	-1.45	-1.46	-1.70	-1.21	2.09	2.09	1.82	2.37
R 0°	-1.27	-1.29	-1.61	-0.95	2.22	2.24	1.89	2.57
R +45°	-1.62	-1.65	-2.07	-1.20	2.33	2.35	1.91	2.79
R +90°	-1.68	-1.70	-2.03	-1.37	1.50	1.52	1.16	1.85

Discussion

The orientation dependence of face identity recognition offers a unique empirical opportunity to address potential retinotopic biases in face identity representations. Through the systematic quantification of the orientation tuning parameters across stimulus rotation, the present study thus enabled a direct test of the reference frame of human face identity recognition.

Overall human sensitivity to face identity was best for upright faces and decreased as a function of face rotation angle in agreement with previous studies (Jacques & Rossion, 2007; Rossion, 2008; see Rossion & Boremanse, 2008 for a review). Despite this overall downward shift in recognition sensitivity, the relative Gaussian tuning profile was largely stable, with comparable peak location, base amplitude and standard deviation across stimulus rotation angles. In other words, identity recognition kept tuned to the horizontal range with comparable sharpness and comparable floor performance in the vertical range.

The large standard deviations of the modelled Gaussians indicate that the horizontal tuning of face identity recognition is broad, in line with past studies that used ‘ambient’ images, i.e., stimuli retaining some ecological variability in face appearance (e.g., in viewpoint, outline and/or lighting; Dumont, Roux-Sibilon, & Goffaux, 2024; Goffaux & Greenwood, 2016; Roux-Sibilon et al., 2025). In these more naturalistic stimuli, the orientation range containing identity-diagnostic cues such as eye and brows may spread to close-to-horizontal oblique ranges (Roux-Sibilon et al., 2025). Moreover, since familiar identity recognition relies not only on stable (horizontal) identity cues but also on the way a face idiosyncratically varies across encounters (e.g., Burton et al., 2016; Ritchie & Burton, 2017), such broad horizontal tuning may provide optimal access to both the stable and idiosyncratically-variable cues to face identity.

While identity recognition performance was broadly tuned to the horizontal range irrespective of stimulus rotation, peak amplitude, i.e., the recognition advantage of horizontal over vertical information, was significantly smaller for ±90° than for ±45° and 0° rotation angles. This indicates that the overall drop of face identity recognition with stimulus rotation found here and in past studies (e.g., Jacques & Rossion, 2007; Rossion & Boremanse, 2008) is due to the impaired processing of horizontal face cues.

Past studies have used a similar approach to compare the orientation tuning profile of identity recognition in upright, contrast-negated, and inverted faces (Dakin & Watt, 2009; Dumont, Roux-Sibilon, & Goffaux, 2024; Goffaux & Greenwood, 2016; Jacques, Schiltz, & Goffaux, 2014), and across viewpoints (Roux-Sibilon et al., 2025). The study by Roux-Sibilon and colleagues (2025) proved the sensitivity of this approach to capture peak location shifts for identity recognition across views with similar sample size, numbers of trials, and orientation filter standard deviation to here.

The stability of the horizontal preference for identity recognition despite face rotation (up to ±90°) confirms that the horizontal information primarily driving human face identity recognition is best defined in a face-centered reference frame. The orientation tuning of face recognition thus reflects the diagnosticity of the information oriented orthogonally to the vertical elongation axis of the human face, irrespective of its orientation when imprinting the observer’s retina. The functional importance of horizontal face information is thus linked to the natural statistics of the upright human face and not to its retinotopic projection.

While our results demonstrate its non-retinotopic, high-level and face-centered nature, they do not exclude the possibility that the horizontal tuning of face identity recognition emerges based on functional interactions across visual processing levels, including the primary visual cortex (V1; de-Wit et al., 2012; Schuurmans et al., 2023). Orientation selectivity is a core functional property of V1 and past evidence shows this function is not limited to the early and static orientation filtering of visual input; instead V1 orientation-selective encoding is a dynamic and protracted process (Ringach, Hawken, & Shapley, 1997, 2003) likely operating under the top-down influence of internal representations, unconstrained by retinotopy (de-Wit et al., 2012; Hsieh et al., 2010; Williams et al., 2008).

Our study focused on disentangling the retino- and face-centered coordinate systems of face identity information but discarded another fundamental reference frame: the one relative to the space in which the stimulus is viewed and/or to the directional pull of gravity, i.e. the environmental reference frame. Few studies rotated both the observer and the stimulus to address whether human face perception operates in an environmental coordinate system. Evidence for the environmental influence on human face perception is scarce and weak (Davidenko & Flusberg, 2012; de Schonen, Leone, & Lipshits, 1998; Lobmaier & Mast, 2007; Troje, 2003). We thus think that this frame of reference is unlikely to contribute to our results.

Although identity recognition kept tuned to the horizontal range irrespective of face rotation, the magnitude of the horizontal advantage over vertical (i.e., peak amplitude) decreased for extreme ±90° rotations. It is unlikely that such reduction in peak amplitude resulted from a floor effect in the vertical range preventing the downward shifting of the full psychometric curve. Indeed, accuracy in the vertical range was well above chance level for ±90° rotations (See Supplementary S1). Instead, we believe that the reduced tuning peak amplitude of face identity recognition for ±90° rotations observed here results at least in part from the disruption of face-specialized holistic processing, namely the perceptual integration of local facial features into a global representation of face identity (e.g., Farah, Tanaka, & Drain, 1995; Farah et al., 1998; Rossion, 2008). Past evidence of face recognition deficit at ±90° of rotation has been attributed to the disruption of specialized holistic processing (Edmonds & Lewis, 2007; Jacques & Rossion, 2007; Jiang, Blanz, & Rossion, 2011; McKone, 2004; McKone, Martini, & Nakayama, 2001; Rossion, 2008; Rossion & Boremanse, 2008) and our past work indicates that the holistic processing of faces is mainly driven by horizontal face cues (Goffaux & Dakin, 2010). However, the selectivity of the recognition impairment to the horizontal range for ±90° face rotations may alternatively reflect a more fundamental contribution of the horizontal face information namely the carriage of the natural statistics of the upright human face that are essential at triggering the visual mechanisms that are specialized to this category (Dakin & Watt, 2009; Dumont, Roux-Sibilon, & Goffaux, 2024; Goffaux et al., 2016; Jacques, Schiltz, & Goffaux, 2014).

To conclude, we leveraged the orientation dependence of identity recognition to quantify the influence of retinotopic mechanisms on the representation of face identity. Our results demonstrate that human face identification stays horizontally-tuned irrespective of stimulus rotation and therefore suggest that face identity information is defined in a face-centered reference frame in agreement with the notion that the horizontally-driven visual mechanisms supporting face-specialized identity recognition are tuned to the natural statistics of the upright face.

Acknowledgments

We thank Ece Kurnaz for her help with data acquisition. We would also like to thank Alexia Roux-Sibilon and Mehmet Umut Canoluk for their help with data analysis.

Author contributions

Funding

This work was supported by the FNRS ASP grants n°: 1.A.681.22F granted to HD and the Excellence of Science grant HUMVISCAT- 30991544. VG is an F.R.S.-F.N.R.S. Research Associate.

References

Afraz, S. R., & Cavanagh, P. (2008). Retinotopy of the face aftereffect. *Vision Res*, *48*(1), 42-54. https://doi.org/10.1016/j.visres.2007.10.028

Balas, B., Huynh, C., Saville, A., & Schmidt, J. (2015). Orientation biases for facial emotion recognition during childhood and adulthood. *Journal of experimental child psychology*, *140*, 171-183. https://doi.org/10.1016/j.jecp.2015.07.006

Balas, B. J., Schmidt, J., & Saville, A. (2015). A face detection bias for horizontal orientations develops in middle childhood. *Front Psychol*, *6*, 772. https://doi.org/10.3389/fpsyg.2015.00772

Bürkner, P. C. (2018a). Advanced Bayesian Multilevel Modeling with the R Package brms. *R Journal*, *10*, 395-411. https://doi.org/10.32614/RJ-2018-017

Bürkner, P. C. (2018b). brms: An R Package for Bayesian Multilevel Models Using Stan. *Journal of Statistical Software*, *80*(1), 1-28. https://doi.org/10.18637/jss.v080.i01

Burton, A. M., Kramer, R. S., Ritchie, K. L., & Jenkins, R. (2016). Identity From Variation: Representations of Faces Derived From Multiple Instances. *Cogn Sci*, *40*(1), 202-223. https://doi.org/10.1111/cogs.12231

Dakin, S. C., & Watt, R. J. (2009). Biological "bar codes" in human faces. *J Vis*, *9*(4), 2 1-10. https://doi.org/10.1167/9.4.2

Davidenko, N., & Flusberg, S. J. (2012). Environmental inversion effects in face perception. *Cognition*, *123*(3), 442-447. https://doi.org/10.1016/j.cognition.2012.02.009

de-Wit, L. H., Kubilius, J., Wagemans, J., & Op de Beeck, H. P. (2012). Bistable Gestalts reduce activity in the whole of V1, not just the retinotopically predicted parts. *J Vis*, *12*(11). https://doi.org/10.1167/12.11.12

de Schonen, S., Leone, G., & Lipshits, M. (1998). The face inversion effect in microgravity: is gravity used as a spatial reference for complex object recognition? *Acta Astronaut*, *42*(1-8), 287-301. https://doi.org/10.1016/s0094-5765(98)00126-x

Dumont, H., Roux-Sibilon, A., & Goffaux, V. (2024). Horizontal face information is the main gateway to the shape and surface cues to familiar face identity *PLOS ONE*.

Duncan, J., Gosselin, F., Cobarro, C., Dugas, G., Blais, C., & Fiset, D. (2017). Orientations for the successful categorization of facial expressions and their link with facial features. *J Vis*, *17*(14), 7. https://doi.org/10.1167/17.14.7

Duncan, J., Royer, J., Dugas, G., Blais, C., & Fiset, D. (2019). Revisiting the link between horizontal tuning and face processing ability with independent measures. *Journal of experimental psychology. Human perception and performance*, *45*(11), 1429-1435. https://doi.org/10.1037/xhp0000684

Edmonds, A. J., & Lewis, M. B. (2007). The effect of rotation on configural encoding in a face-matching task. *Perception*, *36*(3), 446-460. https://doi.org/10.1068/p5530

Farah, M. J., Tanaka, J. W., & Drain, H. M. (1995). What causes the face inversion effect? *Journal of Experimental Psychology: Human Perception and Performance*, *21*(3), 628-634. http://www.ncbi.nlm.nih.gov/entrez/query.fcgi?cmd=Retrieve&db=PubMed&dopt=Citation&list_uids=7790837

Farah, M. J., Wilson, K. D., Drain, M., & Tanaka, J. N. (1998). What is "special" about face perception? *Psychol Rev*, *105*(3), 482-498. https://doi.org/10.1037/0033-295x.105.3.482

Goffaux, V., & Dakin, S. C. (2010). Horizontal information drives the behavioral signatures of face processing. *Front Psychol*, *1*, 143. https://doi.org/10.3389/fpsyg.2010.00143

Goffaux, V., Duecker, F., Hausfeld, L., Schiltz, C., & Goebel, R. (2016). Horizontal tuning for faces originates in high-level Fusiform Face Area [Article de recherche] [peer-

reviewed]. *Neuropsychologia*, *81*(29), 1-11. https://doi.org/10.1016/j.neuropsychologia.2015.12.004
Goffaux, V., & Greenwood, J. A. (2016). The orientation selectivity of face identification [Article de recherche] [peer-reviewed]. *Scientific Reports*, *6*(34204), 34204. https://doi.org/10.1038/srep34204
Groen, I. I. A., Dekker, T. M., Knapen, T., & Silson, E. H. (2022). Visuospatial coding as ubiquitous scaffolding for human cognition. *Trends Cogn Sci*, *26*(1), 81-96. https://doi.org/10.1016/j.tics.2021.10.011
Holler, J. (2025). Facial clues to conversational intentions. *Trends Cogn Sci*, *29*(8), 750-762. https://doi.org/10.1016/j.tics.2025.03.006
Huynh, C. M., & Balas, B. (2014). Emotion recognition (sometimes) depends on horizontal orientations. *Attention, perception & psychophysics*. https://doi.org/10.3758/s13414-014-0669-4
Jacobs, C., Petras, K., Moors, P., & Goffaux, V. (2020). Contrast versus identity encoding in the face image follow distinct orientation selectivity profiles [Article de recherche] [peer-reviewed]. *PLOS ONE*, *15*(3), e0229185. https://doi.org/10.1371/journal.pone.0229185
Jacques, C., & Rossion, B. (2007). Early electrophysiological responses to multiple face orientations correlate with individual discrimination performance in humans. *NeuroImage*, *36*(3), 863-876. https://doi.org/10.1016/j.neuroimage.2007.04.016
Jacques, C., Schiltz, C., & Goffaux, V. (2014). Face perception is tuned to horizontal orientation in the N170 time window [Article de recherche] [peer-reviewed]. *Journal of Vision*, *14*(2), 1-18. https://doi.org/10.1167/14.2.5
Jiang, F., Blanz, V., & Rossion, B. (2011). Holistic processing of shape cues in face identification: Evidence from face inversion, composite faces, and acquired prosopagnosia. *Visual Cognition*, *19*(8), 1003-1034. https://doi.org/10.1080/13506285.2011.604360
Kruschke, J. K., & Liddell, T. M. (2018). Bayesian data analysis for newcomers. *Psychonomic bulletin & review*, *25*(1), 155-177. https://doi.org/10.3758/s13423-017-1272-1
Lobmaier, J. S., & Mast, F. W. (2007). The Thatcher illusion: rotating the viewer instead of the picture. *Perception*, *36*(4), 537-546. https://doi.org/10.1068/p5508
McKone, E. (2004). Isolating the special component of face recognition: peripheral identification and a Mooney face. *J Exp Psychol Learn Mem Cogn*, *30*(1), 181-197. https://doi.org/10.1037/0278-7393.30.1.181
McKone, E., Martini, P., & Nakayama, K. (2001). Categorical perception of face identity in noise isolates configural processing. *Journal of experimental psychology. Human perception and performance*, *27*(3), 573-599. https://doi.org/10.1037//0096-1523.27.3.573
Morsi, A. Y., Goffaux, V., & Greenwood, J. A. (2024). The resolution of face perception varies systematically across the visual field. *PLOS ONE*, *19*(5), e0303400. https://doi.org/10.1371/journal.pone.0303400
Pachai, M. V., Bennett, P. J., & Sekuler, A. B. (2018). The Bandwidth of Diagnostic Horizontal Structure for Face Identification. *Perception*, *47*(4), 397-413. https://doi.org/10.1177/0301006618754479
Pachai, M. V., Sekuler, A. B., & Bennett, P. J. (2013). Sensitivity to Information Conveyed by Horizontal Contours is Correlated with Face Identification Accuracy. *Front Psychol*, *4*, 74. https://doi.org/10.3389/fpsyg.2013.00074

Pachai, M. V., Sekuler, A. B., Bennett, P. J., Schyns, P. G., & Ramon, M. (2017). Personal familiarity enhances sensitivity to horizontal structure during processing of face identity. *J Vis*, *17*(6), 5. https://doi.org/10.1167/17.6.5
Ringach, D. L., Hawken, M. J., & Shapley, R. (1997). Dynamics of orientation tuning in macaque primary visual cortex [Research Support, Non-U.S. Gov't

Research Support, U.S. Gov't, P.H.S.]. *Nature*, *387*(6630), 281-284. https://doi.org/10.1038/387281a0
Ringach, D. L., Hawken, M. J., & Shapley, R. (2003). Dynamics of orientation tuning in macaque V1: the role of global and tuned suppression [Research Support, Non-U.S. Gov't

Research Support, U.S. Gov't, P.H.S.]. *Journal of neurophysiology*, *90*(1), 342-352. https://doi.org/10.1152/jn.01018.2002
Ritchie, K. L., & Burton, A. M. (2017). Learning faces from variability. *Quarterly journal of experimental psychology*, *70*(5), 897-905. https://doi.org/10.1080/17470218.2015.1136656
Rossion, B. (2008). Picture-plane inversion leads to qualitative changes of face perception. *Acta Psychologica*, *128*, 274-289.
Rossion, B., & Boremanse, A. (2008). Nonlinear relationship between holistic processing of individual faces and picture-plane rotation: evidence from the face composite illusion. *J Vis*, *8*(4), 3 1-13. https://doi.org/10.1167/8.4.3
Roux-Sibilon, A., Dumont, H., Bremhorst, V., Jacobs, C., & Goffaux, V. (2025). The view-tolerance of human identity recognition depends on horizontal face information [Reviewed preprint]. *Elife*. https://doi.org/https://doi.org/10.7554/eLife.108495.1
Roux-Sibilon, A., Peyrin, C., Greenwood, J. A., & Goffaux, V. (2023). Radial bias in face identification. *Proc Biol Sci*, *290*(2001), 20231118. https://doi.org/10.1098/rspb.2023.1118
Schuurmans, J. P., Bennett, M. A., Petras, K., & Goffaux, V. (2023). Backward masking reveals coarse-to-fine dynamics in human V1. *NeuroImage*, *274*, 120139. https://doi.org/10.1016/j.neuroimage.2023.120139
Troje, N. F. (2003). Reference frames for orientation anisotropies in face recognition and biological-motion perception. *Perception*, *32*(2), 201-210. https://doi.org/10.1068/p3392
Yu, D., Chai, A., & Chung, S. T. L. (2018). Orientation information in encoding facial expressions. *Vision Res*, *150*, 29-37. https://doi.org/10.1016/j.visres.2018.07.001